ASDEX Simulation Calculations with Simple Transport Laws

Karl Lackner, Otto Gruber,
Reinhard Wunderlich

IPP 5/28 August 1989

MAX-PLANCK-INSTITUT FÜR PLASMAPHYSIK

8046 GARCHING BEI MÜNCHEN

MAX-PLANCK-INSTITUT FÜR PLASMAPHYSIK

GARCHING BEI MÜNCHEN

ASDEX Simulation Calculations with Simple Transport Laws

Karl Lackner, Otto Gruber,
Reinhard Wunderlich

IPP 5/28 August 1989

Die nachstehende Arbeit wurde im Rahmen des Vertrages zwischen dem Max-Planck-Institut für Plasmaphysik und der Europäischen Atomgemeinschaft über die Zusammenarbeit auf dem Gebiete der Plasmaphysik durchgeführt.

Abstract:

Anhand einfacher Ansätze über die Orts- ,Temperatur- und Dichteabhängigkeit anomaler Transportgesetze wird die Frage untersucht, ob die beobachtete Dichteunabhängigkeit der globalen Energieeinschlußzeit in NBI-geheizten Tokamakentladungen durch Depositionseffekte und durch den Anteil schneller Teilchen am Plasmaenergieinhalt hervorgerufen werden kann. 1-d Simulationsrechnungen mit dem BALDUR-Code für ASDEX-Parameter zeigen, daß die letzteren beiden Effekte beträchtlich sein können, und daß aus dort gewonnenen globalen Einschlußzeiten in NBI-geheizten Plasmen kein Widerspruch zu den von elektrostatischen Turbulenztheorien im stoßfreien Regime vorhergesagten Temperatur- und Dichteabhängigkeiten hergeleitet werden kann.

ASDEX SIMULATION CALCULATIONS WITH SIMPLE TRANSPORT LAWS

K.Lackner, O. Gruber, R. Wunderlich

Max-Planck Institut für Plasmaphysik, EURATOM-Association
D 8046 Garching

1. Introduction

Simulation calculations for tokamak discharges have generally been carried out using, for the description of energy and particle transport, either exact expressions derived from first principle theories, or completely ad-hoc postulated formulas, iteratively modified to give a satisfactory fit to experimental results. The first approach, although corresponding to the ultimately desired situation, has so far met only modest success, whereas the outcome of calculations of the second type is of only limited usefulness for the extrapolation to future devices, and raises in particular severe questions of its uniqueness.

To guide the selection of first principle theories to be used in simulation calculation or to be followed up in further theoretical work, one usually translates these local transport laws into global confinement time expressions and compares the predicted dependencies of τ_E on heating power (P_{tot}), line-average electron density ($\overline{n_e}$) and other integral parameters with the experimental observations. This can be however quite misleading, as the actual parameter profiles, and in particular the quoted experimental confinement times depend on a number of other processes besides the energy and particle diffusivities:

- the power deposition profile and its distribution over electrons and ions. This includes both positive (heating power) and negative (radiation losses) contribution (see also ref. /1/) .

- the contribution of non-thermal particles. Frequently confinement times quoted are based on the magnetically determined plasma energy content, which includes also that of fast particles. For mid-size and large tokamaks the latter is presumably not determined by their loss but rather their slowing down rate. As the latter has a dependence on density and plasma temperature opposite to that predicted by most micro-turbulence based energy transport models, the variation of the fast particle energy contribution can partly cloud that of the thermal particles even in situations where their contribution is small but strongly varying over the range of the experimental parameter scan.

On the other hand, these effects can be readily estimated from 1-d transport simulation calculations, which at the same time can also answer to what extent the observed resilience of the electron temperature profile shape to discharge conditions (other than the value of the safety factor at the boundary, q_a) is caused by trivial effects like the shift in the power deposition from

the ion to the electron channel, or an increase in the relative importance of the ohmic contribution to the heating power profiles.

It is therefore illustrative to carry through sets of simulation calculations with simple models of radius-, density- and temperature-dependent transport laws to establish deviations from the expected relation between local and global confinement trends arising from the effects described above. Trigger for the present calculations was the observation that a heat transport law based on a plateau type scaling /2/ gives an overall good fit to the confinement trends over a wide range of machine sizes and discharge parameters, but on the other hand does not correctly reproduce the variation of $\tau_E(\overline{n_e})$ in density scans with NBI-heated discharges on ASDEX. The hypothesis tested here is that these deviations arise from the changes of the power deposition profile and of the contribution of fast particles to the energy content. The results are however also of general relevance for collisionless micro-instabilities /3/, /4/, /4/, which all suffer from such an apparent discrepancy with observations.

The following sections describe sets of such simulation calculations. They correspond to fictitious density and heating power scans, but use realistic parameter ranges, device properties and NBI-system specifications of ASDEX. They aim to describe only Ohmic and L-regime discharges and are restricted in additional heating to neutral injection, for which a validated power deposition model is readily available.

The Princeton-developed BALDUR code /6/ was used for carrying out the simulations. Impurities were generally ignored, by taking into account only bremsstrahlung radiative losses and assuming, except in the section 4, $Z_{eff}=1$. Contributions to transport always included were the neoclassical ion heat conductivity as given by Chang-Hinton /7/, and a Bohm-like enhancement of diffusivities over the region with $q \leq 1$. For the simulations reported here, anomalous contributions $\chi_{e,i,\,anom}$ to the heat diffusivities of ions and electrons were always taken to be of equal functional form, with temperature dependent terms evaluated, however, at the respective species temperature.

Particle transport was taken into account in the calculations, including the refuelling by the beam ions. For each of the transport assumptions tested, we took a particle diffusivity D equal to 1/4 χ_e, and an inward drift velocity $v_{in} = 3 \cdot (D/a) \cdot (r/a)^2$. The latter assumption ensures that the density profiles will tend to $n_{e,as}(r) = n_{eo} \cdot \exp(-(r/a)^3)$ to the extend that sources in the interior region are negligible. The line-average density is feed-back controlled by an adjustable gas-puff to a prescribed value. As we do, at the same time, maintain a constant recycling coefficient (0.9), the feedback system cannot prevent - at low initial densities and high heating powers - a density increase due to beam refuelling. In our simulated density scans, where we always plot quasistationary parameters against actual line- average densities, this leads to an inaccessible region at low densities/high heating powers, in qualitative analogy to the actual experimental situation. As our concern here is with the apparent scaling of confinement time with power and density we do not discuss the poloidal or toroidal field dependence of energy transport.

2. Density and temperature-independent heat diffusivities.

According to the dimensional relation $\tau_E \sim a^2/\chi$, and the power balance relation

$$P_{tot} = 6\pi^2 R_o a^2 \langle nkT \rangle / \tau_E$$

a heat diffusivity

$$\chi \sim T^{\theta} n^{\nu} / B^{j}$$

should give rise to a global confinement time scaling like

$$\tau_E \sim n^{\frac{\theta-\nu}{1+\theta}} \cdot P^{-\frac{\theta}{1+\theta}} \cdot B^{\frac{j}{1+\theta}} \qquad \ldots (1)$$

if other transport effects, or changes in the heat deposition profiles were playing no part. A density and temperature independent χ would therefore also give rise to a density and power independent energy confinement time.

For the simplest study of the effect of penetration and fast particle effects onto global energy confinement we therefore used a heat diffusivity

$$\chi_{anom} = 2.25 \text{ m}^2/\text{s}.$$

Contrary to the simple prediction of equ. (1), a density scan at a constant injected heating power of 2.7 MW gave a significant density dependence of $\tau_{E,tot} = (W_{kin} + W_{beam}) / P_{abs}$ approximately proportional to $\overline{n}^{-0.57}$ and of $\tau_{E,kin} = W_{kin} / P_{abs}$ approximately proportional to $\overline{n}^{-0.35}$ (fig.1).

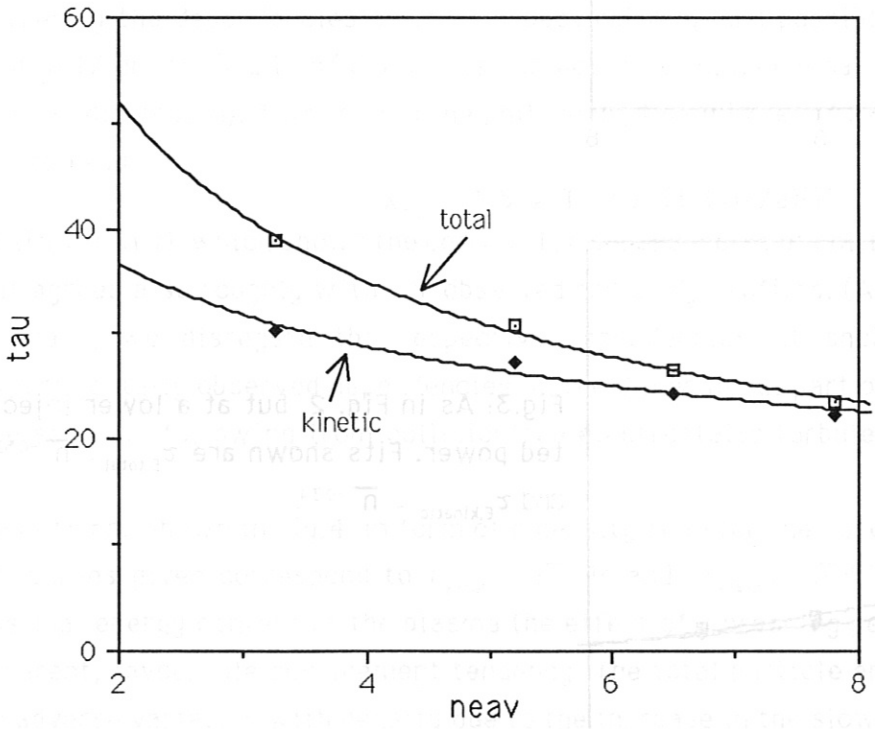

Fig.1

Fig.1: Energy confinement times (in ms) based on the kinetic and total particle energy content, respectively, as predicted by simulations with a spatially constant, parameter independent, anomalous heat diffusivity in a density scan (neav = $\overline{n}/10^{19}$m^{-3}) at 2.7 MW injected NB power. Fits shown are $\tau_{E,total} \sim \overline{n}^{-0.57}$ and $\tau_{E,kinetic} \sim \overline{n}^{-0.35}$.

This density dependence is moreover strongly enhanced if we impose a radial profile on χ_{anom} corresponding roughly to that of χ_e derived from TRANSP-analyses of L-mode shots. For

$$\chi_{anom} = 1.5 /(1.1 - (r/a)^2)\ m^2/s$$

we get at the same power level $\tau_{E'tot} \sim \overline{n}^{-0.8}$ and $\tau_{E'kin} \sim \overline{n}^{-0.56}$, respectively (Fig.2). This is to be expected, as the radially increasing heat diffusivity leads to a more unfavorable weighting of the power deposited in the outer zones, and can also be understood from an inspection of the expression for τ_E in terms of deposition and diffusivity profiles given in the appendix. At lower heating powers, where Ohmic dissipation contributes significantly, the density dependence is weaker. As seen from Fig. 3, we get $\tau_{E'tot} \sim \overline{n}^{-0.53}$ and $\tau_{E'kin} \sim \overline{n}^{-0.34}$ for 1.35 MW injected heating power.

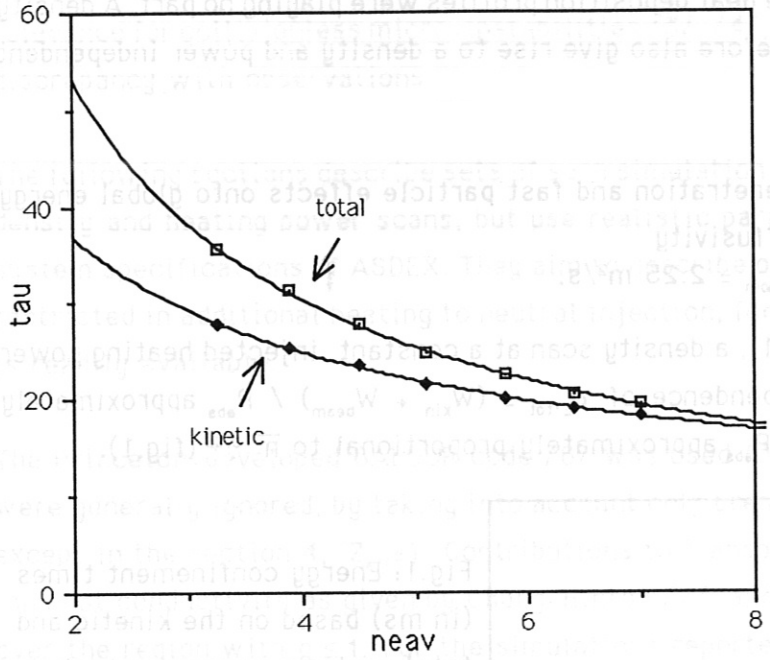

Fig.2

Fig.2: As in Fig. 1, but with a spatially varying diffusivity $\chi_{anom} = 1.5/(1.1-(r/a)^2)\ m^2/s$. Fits shown are $\tau_{E,total} \sim \overline{n}^{-0.8}$ and $\tau_{E,kinetic} \sim \overline{n}^{-0.56}$.

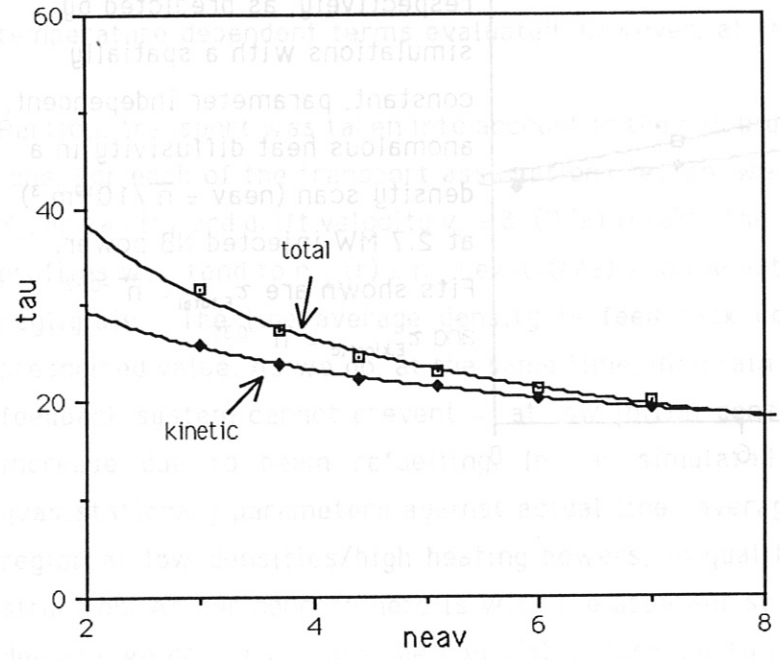

Fig.3

Fig.3: As in Fig. 2, but at a lower injected power. Fits shown are $\tau_{E,total} \sim \overline{n}^{-0.53}$ and $\tau_{E,kinetic} \sim \overline{n}^{-0.34}$.

3. Collisionfree electrostatic turbulence-like T and n dependencies

The above calculations have shown that heat deposition and fast-particle slowing-down effects can give rise to a strong, adverse density dependence of global confinement times even in cases of density and temperature independent heat diffusivities. The question of practical interest is, however, whether diffusivities of the type predicted by strong electrostatic turbulence (collisionless trapped electron and η_i - modes, see ref./7/) in the collisionless regime could give rise to the apparent density independence of τ_E in regimes with strong additional heating.

Such transport models predict

$$\chi \sim T^{3/2}/B^2, \qquad \ldots (2)$$

which according to formula (1) should give rise to

$$\tau_E \sim n^{0.6} P^{-0.6} B^{0.8}$$

in apparent contradiction with experimental observations. Also, in a more local analysis, the theoretical expressions show a radial decrease, rather than an increase of χ. One remedy suggested consists in the superposition of a 'profile-consistency' concept, which is, however, in contradiction with the assumption of a strictly local transport model which we want to test here. We rather assume here that the quantitative theory of strong electrostatic turbulence does not yet give correctly the dependencies on local aspect ratio, q, and possibly other dimensionless ratios like $(r\, d \ln T/ dr)$ or $(r\, d \ln n/ dr)$, but is correct in its dimensional statement $\chi \sim D_{Bohm} \times$ (gyroradius/ plasma dimension). This is also the philosophy taken in ref. / 2/. We have therefore modified equ. (2) to read

$$\chi_{e,i} = 1.5 \times T_{e,i}^{3/2} / (1.1-(r/a)^2)^4 \qquad \ldots(3)$$

(with T in kev), which shows the correct T, n dependencies of collisionfree electrostatic turbulence, but agrees also roughly with our observed radial χ_e-profiles. (As we are not carrying out I_p and B_t - scans, we disregard the respective dependencies. It should be noted however, that the experimentally observed dependencies on the dimensional part of B, Ip are in good agreement with the scalings following from collisionfree electrostatic turbulence models; see also ref. /2/).

Results are shown in Fig.4 in form of a density scan for the case with 2.7 MW injected power. The fit curves given correspond to $\tau_{E,tot} \sim \overline{n}^{-0.12}$ and $\tau_{E,kin} \sim \overline{n}^{-0.16}$, indicating that already for the thermal energy content of the plasma the effect of worsening penetration nearly compensates the inherent, favourable confinement tendency. The total particle energy content, finally, even shows an adverse variation with density due to the increase in the slowing-down time (explicitly through its density and implicitly through its temperature dependence). For comparison we also show the corresponding predictions for the purely Ohmic starting plasmas, for which the density scan, at constant I_p of course does not correspond to a constant power scan. In fact the density dependence found in this case ($\tau_{E,ohm} \sim \overline{n}^{+0.37}$) corresponds nearly exactly to that predicted from equ. (2) under

the constant I_p-constraint ($\tau_{E,ohm} \sim \overline{n}^{+3/8}$).

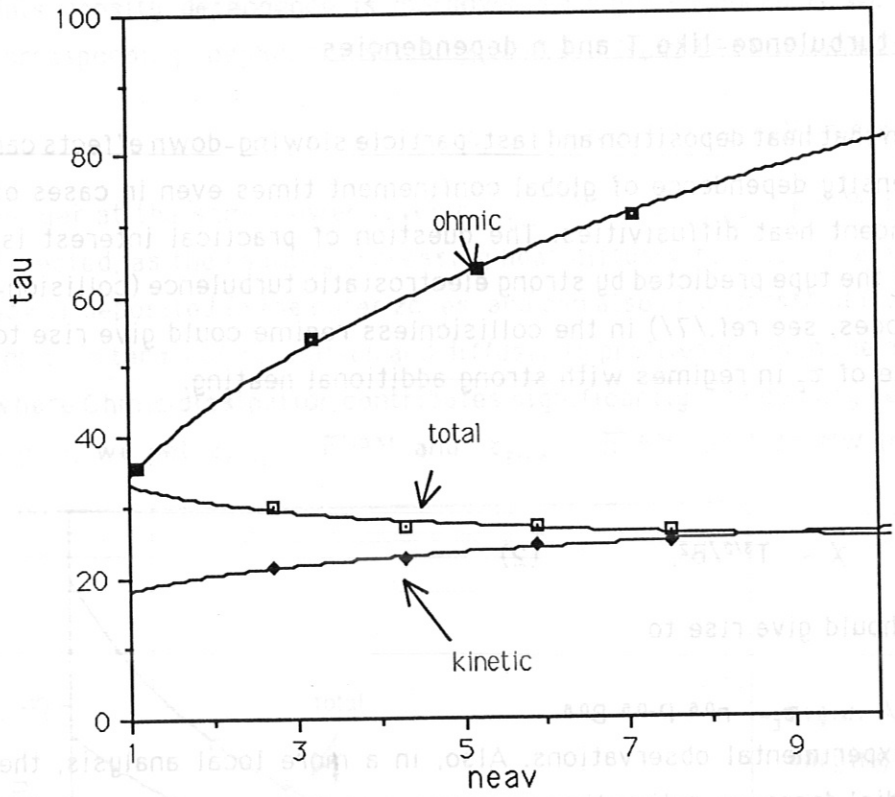

Fig. 4

Fig.4: Energy confinement times (in ms) based on the kinetic and total particle energy content, respectively, as predicted by simulations with anomalous heat diffusivity given by equ. 3 in a density scan under purely Ohmic heating and with 2.7 MW injected NB power. Fits shown are $\tau_{E,total} \sim \overline{n}^{-0.12}$, $\tau_{E,kinetic} \sim \overline{n}^{+0.16}$ and $\tau_{E,ohmic} \sim \overline{n}^{+0.37}$.

We have carried out, with the above transport model, also a power scan at a constant density of $\overline{n} = 5 \times 10^{19}$ m^{-3}, giving, for the kinetic energy indeed the simply predicted $\tau_{E,kin} \sim P^{-0.6}$, but a slightly weaker one, $\tau_{E,total} \sim P^{-0.52}$ for the total energy content (Fig.5). This apparently small difference is of importance when assessing the present experimental data base of measured L-mode confinement times (the so-called 'Kaye(- data base) which is based on magnetic measurements including also fast particles. Taking into account this difference (which for a power scan at lower densities would presumably have been even bigger) it has to be concluded that the fitted power dependencies of such global laws (which, for example, for Goldston/9/ was $\tau_{E,total} \sim P^{-0.5}$) is indeed also in good agreement with the trend predicted by collisionfree electrostatic turbulence.

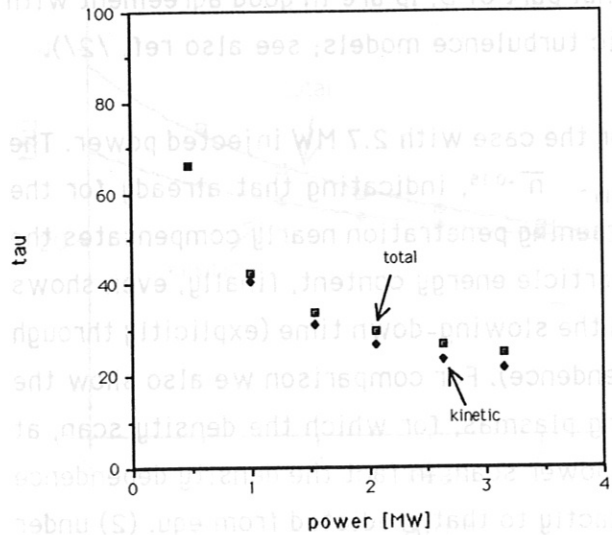

Fig. 5

Fig.5: Energy confinement times (in ms) based on the kinetic and total particle energy content, respectively, as predicted by simulations with an anomalous heat diffusivity given by equ. 3, in a power scan at $\overline{n} = 5 \times 10^{19}$m^{-3}. Fits shown are $\tau_{E,total} \sim P^{-0.6}$, $\tau_{E,kinetic} \sim P^{-0.52}$.

4. Simulation of ASDEX L-mode discharges in H•

The qualitative statements made above suggest also a more quantitative comparison with actual ASDEX L-mode discharges. This is well possible only in hydrogen, as in deuterium the transition into the H-mode limits the parameter space for the L-mode drastically. The experimental results of such a density scan/10/, carried out for B_t = 2.2T, I_p = 300 kA and a constant injected power of 2 MW are presented in Fig. 6.

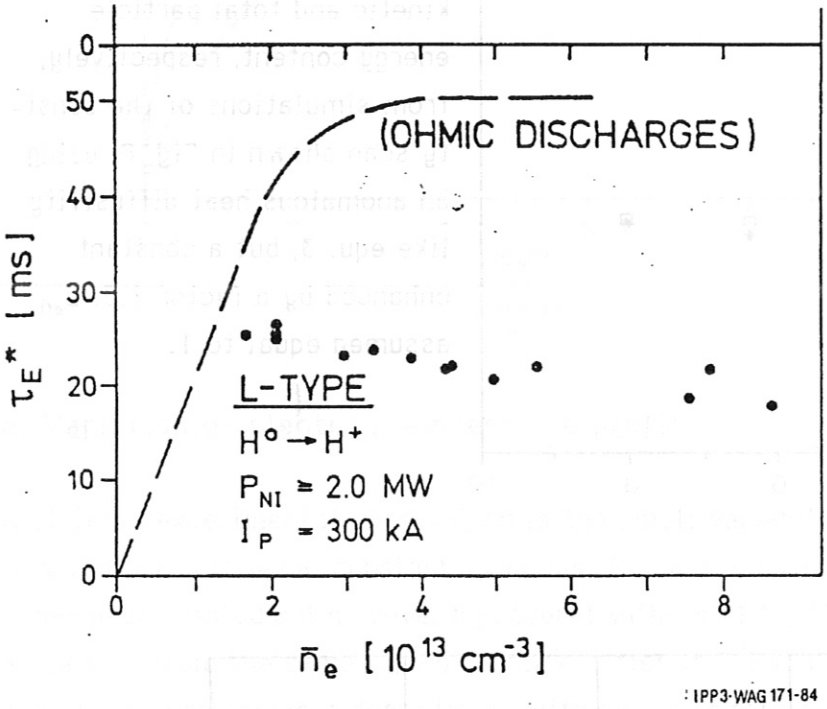

Fig.6: Experimental energy confinement times based on the diamagnetic signal for ASDEX density scans in H• plasmas in Ohmic phase and with 2.0 MW injected NB power.

The corresponding simulations were carried out in two sequences of runs. Both used the anomalous diffusivity like given by equ. 3, albeit with the coefficient raised by a factor 1.5 to account for the worse confinement in hydrogen. In the first set $Z_{eff} \equiv 1$ was assumed throughout. The simulation results for $\tau_{E,total}$ are shown in Fig. 7 and correspond to a quite satisfactory fit for the case with additional heating. In particular, again, nonthermal particles determine the rise of $\tau_{E,total}$ at low densities, as can be seen from the comparison with $\tau_{E,kin}$.

The simulation of the Ohmic cases shows the confinement improvement with density discussed above, which is however weaker, at low densities, than given by the experimental curve, and also does not reproduce the 'hard' saturation at high densities. Using the Ohmic heating constraint: $P_{ohmic} \sim Z_{eff} I_p^2 / T^{3/2}$, a confinement law like equ.3 can be shown to yield (at constant q) $\tau_{E,ohmic} \sim I_p^{1/2} \cdot (n/Z_{eff})^{3/8}$. The experimentally observed systematic increase of Z_{eff} at lower densities (Fig.8, /10/) will thus lead to the observation of a steeper increase of $\tau_{E,ohmic}$ with $\bar{n}$. To quantify this effect, we have fitted the experimental data for Z_{eff} ($\bar{n}$) by a curve $Z_{eff} = 1 + (3.8 \times 10^{19} / \bar{n})^{1.1}$ (solid line in Fig.8) and enforced this variation in a sequence of BALDUR runs with correspondingly controlled C-content. As can be seen from Fig. 9 this procedure indeed leads to a stronger $\tau_E(\bar{n})$ dependence

($\tau_{E,ohmic} \sim \overline{n}^{0.63}$ as the Z_{eff} equal constant case, but again does not reproduce the hard saturation at higher densities. From other analyses /11/, and in particular from the appearance of confinement regimes not showing this saturation (pellet injection and IOC /12/,/13/) it appears clear, however, that the description of this phenomenon requires a more complex physics model than discussed here and also a simultaneous discussion of particle transport.

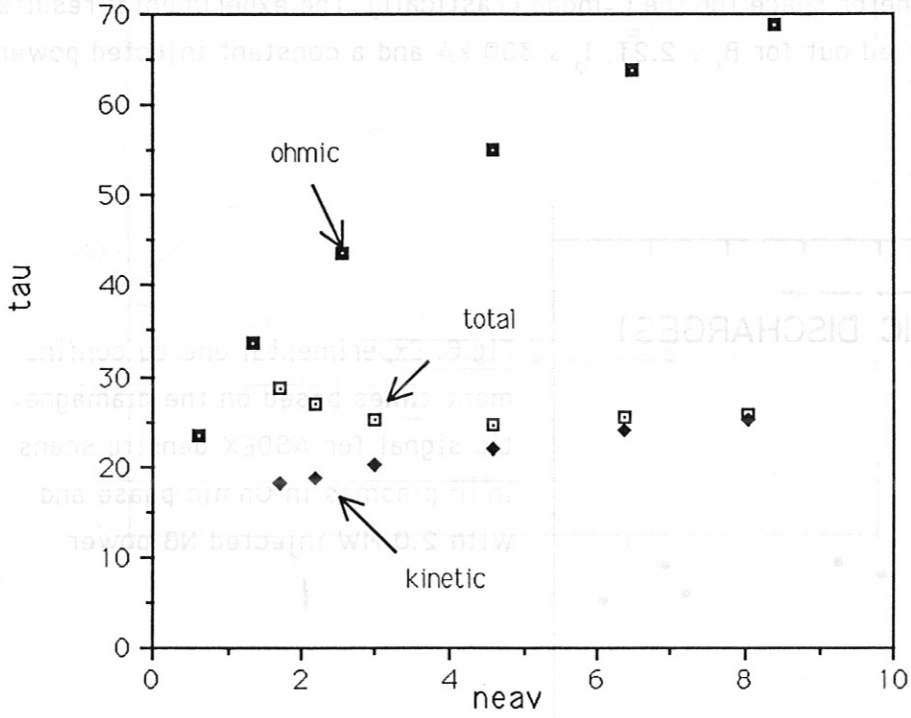

Fig. 7

Fig.7: Energy confinement times (in ms) based on the kinetic and total particle energy content, respectively, from simulations of the density scan shown in Fig. 6, using an anomalous heat diffusivity like equ. 3, but a constant enhanced by a factor 1.5. Z_{eff} assumed equal to 1.

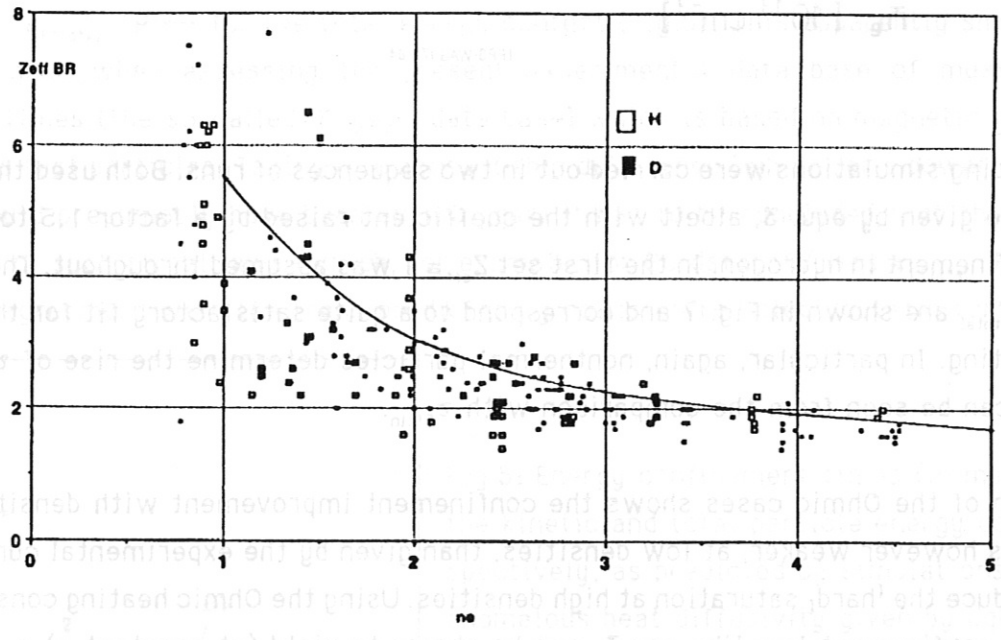

Fig.8: Behaviour of Z_{eff}, as determined from bremsstrahlung, for Ohmically heated ASDEX discharges in H^+ and D^+ plasmas. The fit line shown corresponds to $Z_{eff} = 1 + (3.8 \times 10^{19}/\overline{n})^{1.1}$.

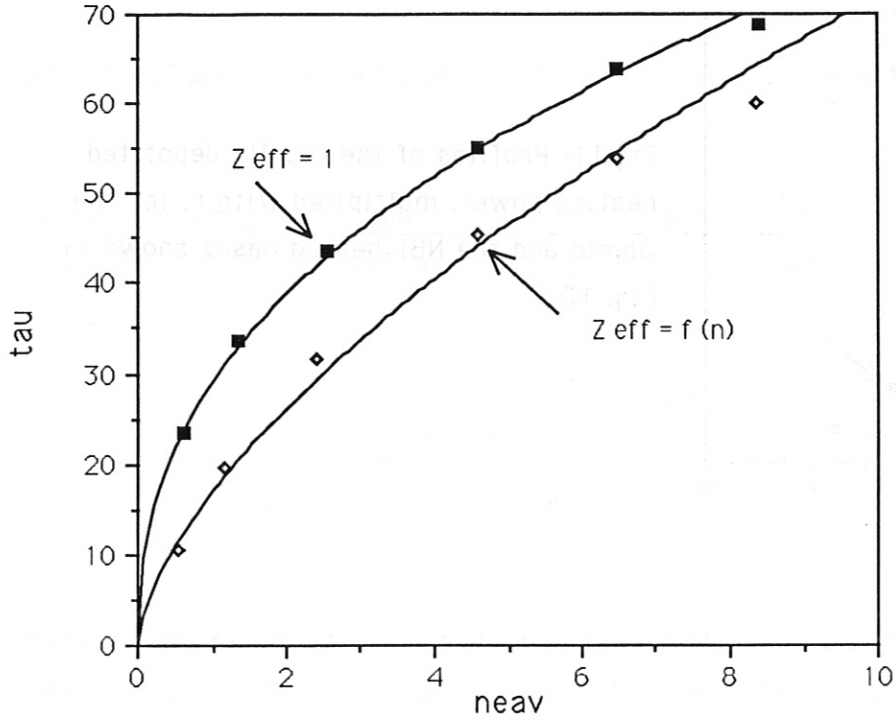

Fig. 9

Fig.9: Energy confinement times (in ms) from simulations of the Ohmically heated discharges of Fig.6, with the heat transport law of Fig. 7, and Z_{eff} taken either as constant or according to the fit of Fig.8.

5. Variation of electron temperature profile

A striking experimental observation is the small variability of the properly normalized electron temperature profiles at constant q_a-values. This has given rise to the concept of profile consistency. It has been pointed out however by several authors /14/, /15/ that a strong resilience of $T_e(r)$ can arise also from the same type of nonlinearities in the transport coefficients that are required to explain the confinement degradation with power in terms of local diffusivities. To illustrate the degree to which this is also the case for the diffusivity ansatz of equation 3, we present the $T_e(r)$-profiles (Fig.10), normalized to their values at r/a = 0.5 for the ohmic and the NBI-heated phase of the highest density case (with $\overline{n_e} = 8 \times 10^{19} m^{-3}$) of the scan used in Fig. 7. The variation is indeed small, considering that the variation in heat deposition profile (Fig.11) corresponds nearly to the practical extremes.

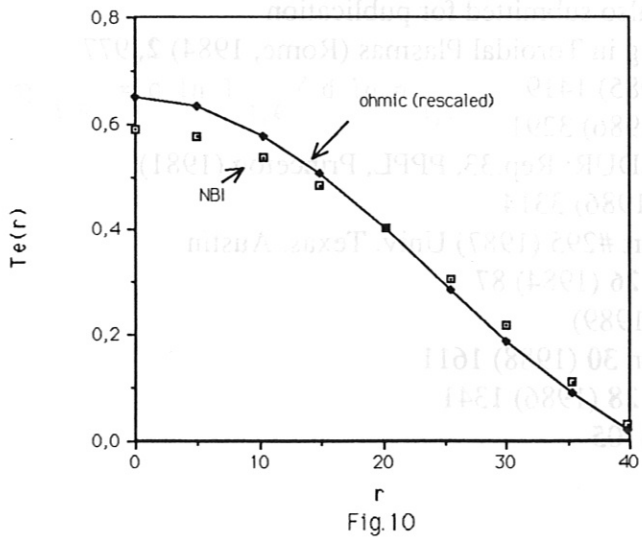

Fig.10

Fig.10: Electron temperature profiles for the highest density case of the sequence shown in Fig.7 during the NBI and the Ohmic phases. The Ohmic profile is rescaled by a factor 1.42 so as to agree with the NBI-heated one at r = 20 cm.

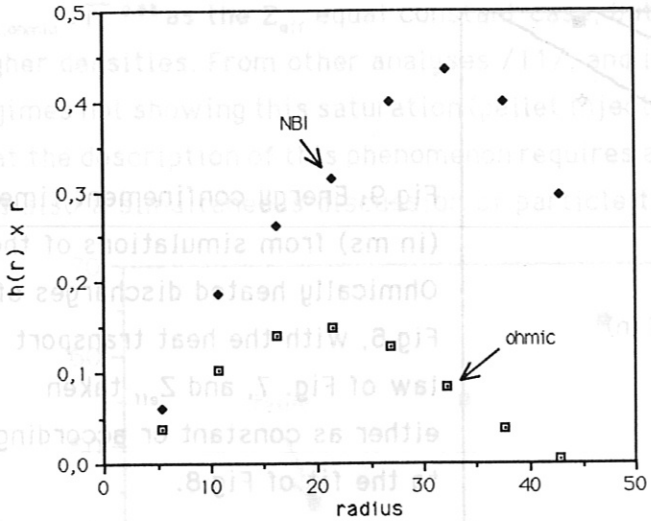

Fig.11

Fig.11: Profiles of the locally deposited heating power, multiplied with r, for the Ohmic and the NBI-heated cases shown in Fig. 10.

6. Conclusions

The simulations reported here show that heat deposition effects and fast particle contributions to the total energy content can significantly affect the apparent scaling of global confinement times with density and power. In particular the weak or absent density dependence of confinement times in NBI-heated discharges needs not necessarily be in contrast with predictions of transport models based on strong electrostatic turbulence in the collisionfree regimes. A consequence of the near cancelling of deposition effects and intrinsic confinement trends would be also a relatively large spread in the exponents α and γ between fits of the form $\tau_{E,tot} \sim n^{\alpha} P_{tot}^{\gamma}$ obtained on different experiments, which would reflect differences in the typical operating regime. Global confinement time analyses in terms of the kinetic energy content alone will be more revealing of the true nature of the underlying transport. Not touched upon in this report was the question of the isotope scaling of energy confinement, which at present remains the most important obstacle to the acceptance of electrostatic turbulence as dominating cause of anomalous heat losses in tokamaks.

References:

/1/ J.D. Callen et al., Nucl. Fusion **27** (1987) 1857
/2/ K.Lackner, N. Gottardi, JET-P(88) 77 (1988), also submitted for publication
/3/ F.W. Perkins, in Proc. 4th Int. Symp. on Heating in Toroidal Plasmas (Rome, 1984) **2**, 977
/4/ P.Terry and P.H. Diamond, Phys. Fluids **28** (1985) 1419
/5/ G.S. Lee and P.H. Diamond, Phys. Fluids **29** (1986) 3291
/6/ D.E. Post, C. E. Singer, A.M. McKenney, BALDUR: Rep.33, PPPL, Princeton (1981)
/7/ C. S. Chang and F.L. Hinton, Phys. Fluids **29** (1986) 3314
/8/ D.W. Ross et al., Fusion Research Center Report #295 (1987) Univ. Texas, Austin
/9/ R.J. Goldston, Plasma Phys. and Contr. Fusion **26** (1984) 87
/10/ F. Wagner and ASDEX Team, private comm. (1989)
/11/ O. Gruber et al., Plasma Phys. and Contr. Fusion **30** (1988) 1611
/12/ M. Kaufmann, Plasma Phys. and Contr. Fusion **28** (1986) 1341
/13/ F.X. Söldner et al., Phys. Rev. Lett. **61** (1988) 1105
/14/ K. Lackner, IPP Report V/14 (1987)
/15/ P.Thomas, JET-P(87) 17 (1987)

Appendix: Connection between Heat Conductivity and Energy Confinement Time

The global energy confinement time $\tau_E = (W_e+W_i) / P_{tot}$ can be connected in the most general stationary case to the heat conductivity and power deposition profiles through the expression

$$\tau_E = \frac{3}{4}\int_0^a \left(\frac{1+\frac{1}{\eta_e}}{\chi_e} H_e(r) + \left(\frac{1+\frac{1}{\eta_e}}{\chi_e} - \frac{1+\frac{1}{\eta_i}}{\chi_i} \right) H_{ie}(r) + \frac{1+\frac{1}{\eta_i}}{\chi_i} H_i(r) \right) r\, dr$$

where $\chi_{i,e}$ are the local ion and electron heat diffusivity coefficients, $H_{i,e}$ are the deposition profiles of direct heating power $h_{e,i}(r)$ in the non-dimensional forms

$$H_{i,e}(r) = \int_0^r h_{i,e}(\rho)\, \rho\, d\rho \;/\; \left(\int_0^a (h_e(\rho) + h_i(\rho))\, \rho\, d\rho \right)$$

and $H_{ie}(r)$ the corresponding measure of the electron-ion energy exchange

$$H_{ie}(r) = \int_0^r h_{ie}(\rho)\, \rho\, d\rho \;/\; \left(\int_0^a (h_e(\rho) + h_i(\rho))\, \rho\, d\rho \right)$$

Radiation losses, in this terminology, would just corrrespond to negative contributions to $h_e(r)$, which should however not be counted in evaluating the denominator of the expressions for $H_{i,e}$ and H_{ie}. $\eta_{i,e}$ has the usual meaning

$$\eta_{i,e} = d \ln T_{i,e} / d \ln n_{i,e}$$